IEEE Access
Multidisciplinary ⋮ Rapid Review ⋮ Open Access Journal

Received 30 November 2023, accepted 18 December 2023, date of publication 1 January 2024,
date of current version 12 January 2024.

Digital Object Identifier 10.1109/ACCESS.2023.3348817

RESEARCH ARTICLE

KONet: Toward a Weighted Ensemble Learning Model for Knee Osteoporosis Classification

M. J. AASHIK RASOOL, (Member, IEEE), SHABIR AHMAD, (Senior Member, IEEE), UMIRZAKOVA SABINA, AND TAEG KEUN WHANGBO, (Member, IEEE)
Department of IT Convergence Engineering, Gachon University, Sujeong-gu, Seongnam-si, Gyeonggi-do 461-701, Republic of Korea

Corresponding author: Taeg Keun Whangbo (tkwhangbo@gachon.ac.kr)

This work was supported by the GRRC Program of Gyeonggi-do Province, Development of Healthcare Contents Based on AI under Grant GRRC-Gachon2021(B03).

ABSTRACT Knee osteoporosis (KOP) is a skeletal disorder characterized by bone tissue degradation and low bone density, leading to a high risk of bone fractures in the knee area. The traditional method for identifying knee osteoporosis is knee radiography, which requires sufficient expertise from specialists. However, the sheer volume of X-rays and the subtle variations among them may lead to misinterpretation. In recent years, deep learning algorithms have revolutionized medical diagnosis and reduced misclassification. Specifically, convolutional neural network (CNN)-based algorithms have been utilized to automate the diagnostic process as they have the inherent ability to extract important features that are difficult to identify manually. However, relying on a single method may result in suboptimal performance, leading to ineffective deployment in the medical domain. To alleviate this issue, in this study, we propose a robust detection method, KONet, which utilizes a weighted ensemble approach to distinguish between normal and osteoporotic knee conditions, even when there are minor variations in the data. To validate the architectural choices in the ensemble approach, we conducted experiments on various state-of-the-art CNN-based models using transfer learning. Extensive experiments indicated that the proposed model achieves a higher accuracy than existing models, outperforming the state-of-the-art models by a significant margin.

INDEX TERMS Convolutional neural network, classification model, knee osteoporosis, skeletal health, transfer learning, weighted ensemble learning.

I. INTRODUCTION

Osteoporosis is a condition that affects the skeletal system and is characterized by a reduction in bone mass and bone tissue degradation, leading to low bone density and an increased risk of bone fractures. A specific manifestation of osteoporosis, known as Knee Osteoporosis (KOP), primarily affects the knee area and has gained increasing attention in recent years, impacting millions of people [1], [2], [3]. The World Health Organization identifies several key risk factors associated with the development of KOP, including age, gender, family history, hormonal imbalances, and lifestyle factors such as excessive alcohol consumption [4]. Women, in particular, are classified as a high-risk group for developing KOP, with numerous studies supporting this assertion [5], [6].

The associate editor coordinating the review of this manuscript and approving it for publication was Dian Tjondronegoro.

KOP conditions are marked by a significant decrease in bone mineral density and alterations in the protein composition of bones, which contribute to the vulnerability of knee bones to fractures and other pathological changes [7], [8]. Typical indications of this disease include persistent discomfort and pain in the affected knee region, stiffness, and reduced mobility, all of which significantly affect an individual's quality of life [4]. It is important to note that KOP is an irreversible and incurable disease; however, timely identification and specific treatments can significantly slow or even halt its progression, improving the overall well-being of affected individuals [7], [9]. The treatment of KOP necessitates a multidisciplinary approach, encompassing pharmacological treatments, lifestyle modifications, and physical therapy [1].

In the realm of pharmacological treatments, options such as bisphosphonates, hormone therapy, and selective estrogen receptor modulators have shown promise in enhancing

bone density and mitigating fracture risk [10]. Furthermore, lifestyle adjustments, including weight-bearing exercises, ensuring adequate calcium and vitamin D intake, and abstaining from smoking and excessive alcohol consumption, play a pivotal role in promoting bone health and the effective management of KOP.

In contemporary healthcare, KOP detection and classification are conducted with the collaboration of medical experts through the examination of images acquired using X-rays, quantitative ultrasound system (QUS), computed tomography (CT) [11], [12], and magnetic resonance imaging (MRI) [13], [14]. Compared to other techniques, X-rays are cost-effective and widely available. X-ray imaging is commonly used in the medical community to diagnose bone pathology [15]. These images are the most widely used methods for identifying fractures or abnormalities in body bones, such as the knee, elbow, wrist, spine, pelvis, and shoulder. However, numerous X-rays and the minor differences between them can lead to misjudgments in KOP identification [16]. To address these issues, efforts have been made over the years to automate the process. For instance, recent studies have suggested a significant shift toward the use of automatic diagnostic systems based on deep learning to assist medical experts [16], [17].

The convolutional neural network (CNN) is the de facto deep learning approach for automatic feature extraction from images and has been utilized to detect several disease conditions, such as pneumonia [18] and breast cancer [19]. Although CNN-based variant models such as ResNet50, AlexNet, VGG19, SqueezeNet, EfficientNet, VGG16, and GoogLeNet, have demonstrated successful outcomes in classifying medical images, they face significant challenges. The primary obstacle lies in the requirement for large amounts of labeled data for training, which can be arduous to acquire in the medical domain [20], and the cost is high. To address this issue, researchers have proposed the concept of transfer learning. In transfer learning [21], a CNN trained on a large dataset is retrained on a novel problem with fewer data, whereby the CNN can quickly learn features on the small new dataset by using the knowledge gained from the large dataset. This method is particularly useful when the data are too few to achieve certain tasks. The pre-trained model provides a better starting point and avoids the retraining of a large model from scratch [21], [22]. This helps to effectively solve various image-classification tasks [21]. Despite the higher performance exhibited by several methodologies in classifying KOP, certain limitations still exist in the proposed methods. In particular, existing methodologies perform better in the training phase; however, their accuracy is clearly lower in the validation and testing phases [16], [17]. In the automated healthcare field, testing accuracy is crucial because a minor increase in accuracy can lead to a more accurate and faster diagnosis, which can improve patient outcomes and treatment plans.

Considering these problems, we propose a method for constructing a weighted ensemble model using a transfer-learning approach to diagnose KOP. The primary objective of this approach is to avoid depending solely on a single method and mitigate the biases and variance present in individual models. This is accomplished using a weighted ensemble technique, which assigns greater weight to the optimal model, thereby combining the capabilities of several models to increase the overall performance. This method has shown promising results compared to other existing approaches. The contributions of this study are summarized as follows:

- Our primary contribution is the development of the KONet model, which seamlessly integrates the strengths of EfficientNetB0 and DenseNet121 through a weighted ensemble approach for KOP diagnosis. To achieve this, we use custom weights to combine the capabilities of both models and enhance overall performance, allowing for adaptive feature selection and representation. The weighted ensemble technique assigns greater importance to the optimal model, mitigating the biases and variance present in individual models. Notably, our KONet model has shown promising results when compared to other existing approaches, making it the first ensemble learning-based approach for KOP classification.
- A thorough evaluation was conducted on various state-of-the-art models, including KONet, and their respective performance measures were analyzed.
- A comprehensive evaluation was performed on various weight configurations to determine the optimal weights that would enhance performance metrics.

The remainder of the paper is organized as follows: Section II presents several related works conducted for disease classification and KOP diagnosis, using visual AI. In Section III, the preliminaries of the proposed approach are outlined. Section IV presents the proposed architecture and provides an overview of the ensemble process and optimization strategy. In Section V, the materials and experimental setup used in the KONet approach are introduced. This section also elucidates some of the pre-processing phases necessary for building the proposed model. Section VI presents a discussion on the performance metric analyses utilized. Section VII concludes the paper and identifies the limitations and future directions of this work.

II. RELATED WORKS

The related works in this paper consist of two distinct components: the role of visual artificial intelligence (AI) in the classification and detection of different diseases and an overview of the state-of-the-art in KOP classification.

A. STATE-OF-THE-ART ON VISUAL AI FOR DISEASE DIAGNOSIS

In response to the rapid transformation of AI, several approaches have been adopted in the healthcare sector to diagnose diseases using computer vision. In particular, after the introduction of CNN approaches, researchers developed

FIGURE 1. Dataset samples with ground truth labels.

disease diagnosis systems utilizing CNN. Farooq et al. [23] introduced a classification method for Alzheimer's disease using MRI images; they utilized GoogLenet, ResNet-18, and ResNet-152. Among these networks, GoogLeNet exhibited 98.88% accuracy. In [24] CheXNet algorithm was developed to distinguish 14 types of diseases by examining chest X-ray images. The network consisted of a 121-layer CNN and was trained on the ChestX-ray14 dataset. They checked the performance of their approach using the annotations of four practicing academic radiologists on a test set and noticed that their system performed better than the average radiologist. Visual AI approaches have been applied to chest radiographs, microscopy images, MRI, and other medical image datasets to help health practitioners. For instance, in [25], an automated segmentation method was proposed to segment brain tumors using a CNN trained on MRI images with promising results; however, because of overfitting, there were fewer parameters. The work that uses the dice similarity coefficient metrics was the result of participating in the brain tumor image segmentation benchmark (BRATS) algorithm challenge, where it secured second place. In addition to MRI, several approaches involving microscopy images, as in [26] have proposed the CapsNet neural network to classify 2D HeLa cells. The authors in [27] developed a method to effectively detect osteoporosis by applying CNNs to oral panoramic radiographs. Herein, patient-specific characteristics in common clinical circumstances considerably boosted the prediction accuracy compared with the image-only mode. This study anticipated that by exploiting the sophisticated inference capabilities of deep learning, key clinical parameters that cannot be identified solely from dental panoramic X-ray images would be considered simultaneously, resulting in improved diagnostic precision [27]. Recently, Ahmad et al. introduced an approach that leverages a modified version of YOLOv7 along with a squeeze-and-excitation network to detect gastric lesions in endoscopic images, classifying them into four distinct categories [28]. This approach initially addressed the four distinct classes and exhibited significantly improved performance. In addition, Konwer et al. proposed an approach to predict the progression of the disease by utilizing analysis of temporal images [29]. Here, the authors' suggested approach includes two main components such as self-attention-based temporal convolutional network (TCN) to acquire disease trajectory representations and a vision transformer that is pre-trained in self-supervised methods to extract features from single-time point medical images. This method demonstrated substantial and statistically significant results in comparison to established methodologies.

B. STATE-OF-THE-ART ON KOP DETECTION AND CLASSIFICATION

In the domain of disease detection, deep learning has demonstrated superior results compared to traditional methods [26]. Several deep-learning approaches have also been used for KOP diagnosis. The authors of [17] proposed a transfer learning method using a VGG16 network for KOP classification. They achieved 88% accuracy with fine-tuning and 80% accuracy without fine-tuning. Five folds were randomly selected from the training dataset to reduce bias and overfitting during training. The fundamental shortcoming

TABLE 1. Analysis of osteoporosis classification approaches.

Approaches	Dataset	Method	Limitations
Usman et al. [17]	From Mendeley knee X-ray osteoporosis database [30]	Constructing VGG16 utilizing transfer learning approach to classify 3 classes	VGG16 is a simple network and it often fails to capture complex structures of medical images.
Usman et al. [16]	The osteoporosis knee X-ray dataset [31]	Constructing GoogLeNet (Inception model) utilizing transfer learning approach to classify binary classes	Inception is a complex network, which also requires substantial resources and leads to overfitting conditions.
K. Hatano et al. [32]	Computed radiography(CR) images of phalanges area (source is not mentioned)	Constructing a classifier based on deep convolutional neural network (DCNN) to classify osteoporosis condition in phalanges area.	This approach is challenging when conducting identification within the region of interest(ROI) using DCNN solely based on textural information.

is the VGG16 network's simplicity, which is insufficient to adequately represent the complicated structures required for identifying the KOP conditions. In [16] transfer learning approaches were compared with several state-of-the-art models, with GoogLeNet achieving 90% accuracy. The authors followed 30 epochs and used the RMSProp optimizer to achieve the results. The GoogLeNet architecture is intricate and demands considerable computational resources, potentially resulting overfitting circumstances. In [32] digital computed radiography images were used to train a DCNN for osteoporosis diagnosis of the phalanges (digital bones in the hands). They used threefold cross-validation to achieve better accuracy in osteoporosis diagnosis. A comparative analysis was conducted to identify KOP conditions. The dataset, methods, and limitations are summarized in Table 1. Apart from these studies, there has been little research using deep-learning algorithms in this domain.

High accuracy is essential in disease identification. Although other domains for diagnosing illnesses have achieved more than 90% accuracy [27], current approaches for KOP detection still demonstrate 90% accuracy. This disparity poses a significant problem requiring a dedicated strategy.

III. PRELIMINARIES

A. TRANSFER LEARNING METHOD

The key idea behind transfer learning for image classification is that a model that is trained on a sufficiently large and general dataset effectively acts as a general model of the visible world, whereby the advantage is the use of acquired feature maps, rather than training a large model on a large dataset to rebuild from scratch [33], [34]. This approach helps to prevent obstacles to domain adaption and improves data efficiency. In transfer learning, two major scenarios exist: using a convolutional network as a fixed-feature extractor and fine-tuning the convolutional network [35]. This study freezes the first 10 layers during the construction of the baseline models, followed by the application of the fine-tuning mechanism.

B. FINE TUNING

Fine-tuning is a method of adapting an architecture to a new task using an existing model on specific datasets. During fine-tuning, the pre-trained weights are updated with new weights [35]. In deep learning, this method is commonly used to update parameters by introducing additional data into an existing model. There are four major scenarios in transfer learning that use standard rules of thumb. In the first scenario, the new dataset is small and similar to the original dataset. In the second scenario, the dataset is large but similar to the original dataset [36], and CNN is preferred as a fixed feature extractor method. In the third scenario, the novel dataset is large and differs from the original dataset, and the CNN method is preferably fine-tuned. Finally, in the fourth case, if the novel dataset is small but differs from the original dataset, the CNN method is preferably fine-tuned. In the proposed approach, we followed the fourth rule as our dataset was considerably smaller than the ImageNet dataset and substantially different. It is evident that in the fourth scenario, which is shown in the rightmost column, the model was fine-tuned by rearranging the final layer to satisfy domain-specific requirements. For instance, the EfficientNetB0 and Densenet121 pre-trained models have 1000 classes, whereas, in the proposed scenario, there are only two classes. Therefore, the architecture must be fine-tuned to satisfy the proposed criteria.

C. BASELINE NETWORK ARCHITECTURES

The EfficientNetB0 and DenseNet121 architectures used in this study demonstrated superior performance on the KOP dataset. The primary reason for selecting these architectures was their superior test accuracy, indicating their capacity for producing more reliable results in the context of our research. We used the transfer learning method and fine-tuned the last ten layers of these architectures to improve accuracy. An approach for realizing this is to reuse an existing network to extract essential features from new samples and incorporate a novel classifier model to make predictions based on the extracted features. However, the studied model is specific to the original classification problem and therefore, specific to the set of classes on which the model has been trained. In our problem, the objectives of the learned feature maps had to be reset for the dataset.

1) DenseNet121 ARCHITECTURE

DenseNet is a well-known architecture that was introduced in 2017 [37]. DenseNet121 has 121 layers and is specifically

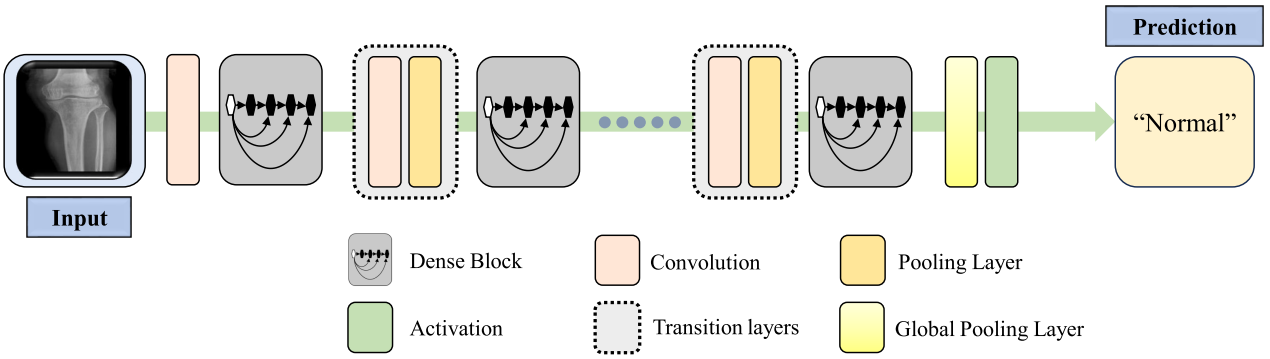

FIGURE 2. Transfer learned DenseNet121 architecture to KOP dataset.

designed for image classification tasks [37]. This model is structured into three key components: dense blocks, transition layers, and classifiers.

The core of DenseNet121 lies in its dense blocks. Dense blocks contain several convolutional layers, each interconnected to all previous layers. Here, dense blocks receive input from all previous layers and maintain constant feature map dimensions while varying the number of filters between them. This intricate connectivity ensures that each layer receives input from all preceding layers. This approach aids in preserving information throughout the network, potentially improving the model's learning capability. It addresses the vanishing gradient issue and leads to improved model accuracy with parameter efficiency. The second part of the network is the transition layer, which performs down-sampling using a combination of convolutional layers and a pooling layer. The third and final part of the network is the classifier [38]. The classifier consists of a global pooling layer, followed by a fully connected layer with an activation function (softmax) that provides the predicted results [39]. The process is demonstrated in Figure 2.

2) EfficientNetB0 ARCHITECTURE

The EfficientNet architecture consists of eight variants such as EfficientNetB0 to EfficientNetB7. The intuition behind this network is on scaling the depth, width, and resolution of the neural network [40]. EfficientNetB0 is a simple and less complex network within the EfficientNet family. It consists of 18 convolution layers. According to Figure 3, initially, the input image size of 224 × 224 passes through the first layer. Subsequent layers decrease in resolution to reduce feature map size while enhancing accuracy [41]. Each layer has channels of 32, 16, 24, 40, 56, 80, 112, 192, 320, and 1280, respectively. On the other hand, the height and width decrease progressively to 112, 56, 28, 14, and 7, respectively. Following the convolutions, this information is forwarded to the fully connected layer, where the maximum number of filters employed is 1280. The final layer is responsible for conducting the classification.

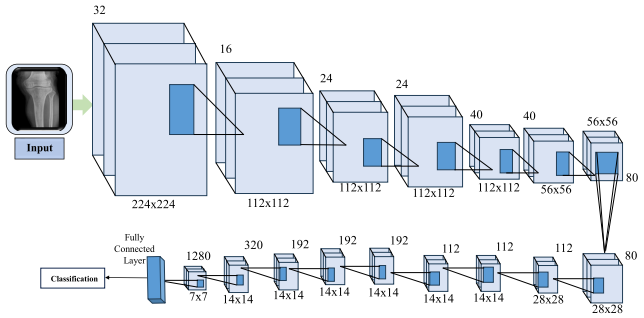

FIGURE 3. Transfer learned EfficientNetB0 architecture to KOP dataset.

D. WEIGHTED ENSEMBLE-LEARNING MODEL

Ensemble learning, a powerful machine learning approach, combines numerous distinct models to generate a new model that improves prediction accuracy for certain tasks. References [42] and [43]. This method has proven to be beneficial in a variety of fields of study [44], [45]. In this study, the weighted ensemble model method was used. The weighted ensemble model approach assigns higher weights to models with better performance on the validation and test datasets. The intuition behind the weighted-average mechanism relies on combining the strengths of several models and reducing their weaknesses. In the proposed weighted ensemble model, each model contributes to the outcome based on its strengths and weaknesses.

In the proposed KONet, we identified the two most optimal models from the pool of trained networks by analyzing the test accuracy of each network. Subsequently, a weighted ensemble model was constructed. Eq. 1 illustrates the ensemble process:

$$\text{Ensemble prediction} = W_1 \cdot M_1 + W_2 \cdot M_2 \qquad (1)$$

where W_1 represents the assigned weight of Model 1, and W_2 represents the weight of Model 2. M_1 denotes the prediction of Model 1, and M_2 represents the prediction of Model 2. The two optimal models that provided better accuracy were selected for the KOP dataset. Different weight ratios were then assigned to these models in constructing an ensemble model. During the construction process,

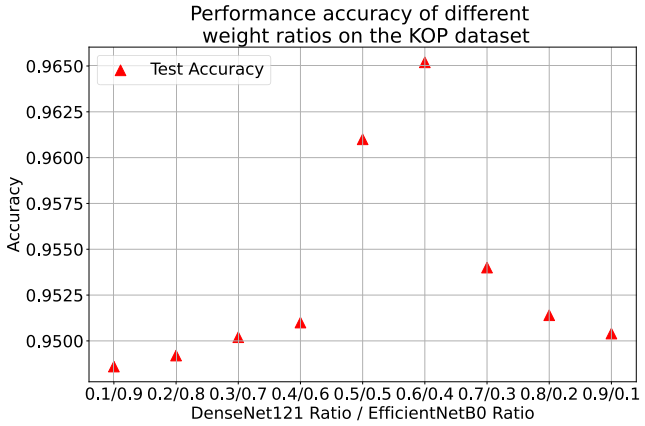

FIGURE 4. Performance accuracy of different weight ratios on the KOP dataset using DenseNet121 and EfficientNetB0 models.

the weights of 0.6 for Densenet121 and 0.4 for EfficientNetB0 exhibited the best performance during the testing phase. In Figure 4, the performance accuracy of different weight ratios on the KOP dataset is presented for the EfficientNetB0 and DenseNet121 models.

IV. PROPOSED APPROACH

In this section, we present the methodology employed in our study and the optimization strategies used to construct KONet.

A. METHODOLOGY

Algorithm 1 and Figure 6 present a comprehensive outline of the workflow adopted in this study. Initially, the data are pre-possessed, and subsequently partitioned into training, test, and validation sets in the ratios of 0.8, 0.1, and 0.1, respectively. The transfer-learning approach was then utilized to construct the six CNN models. In constructing these networks, the first ten layers were frozen and the remaining layers were fine-tuned on our dataset. The transfer learning approach was chosen due to the relatively small size of our dataset, and fine-tuning the last ten layers was necessary because our data differs from the ImageNet dataset. During fine-tuning, the final layer was arranged by applying the linear transformation expressed in Eq. 2 below

$$y = xA^T + b \tag{2}$$

where x represents the incoming data; y represents the output data after transformation; A^T represents the learnable weight of the shape A; b represents the additional bias learned during training. The collection of models is denoted as M_i in the 5th line of Algorithm 1, where each element is represented by $M_1, M_2, M_3, M_4, M_5, M_6$. The models were arranged in descending order based on their test accuracy scores. To accomplish this, the cardinality (number of elements) of the set containing indices i, was calculated with the evaluation score S_i equal to the evaluation score S_k, for each k in the range of 1 to 6.

Subsequently, the 7th line of Algorithm 1 demonstrates that the two optimal models among the trained models, BM_1 (DenseNet121) and BM_2 (EfficientNetB0), were adopted as the best models for further analyses and ensemble construction. When constructing the EfficientNetB0, a dropout ratio of 0.1 was applied. By contrast, in DenseNet121, a dropout ratio of 0.3 was adopted. The dropout technique helps circumvent the overfitting problem.

Algorithm 1 Algorithm for Our Proposed Approach

1: **Preprocess** the data.
2: **Split** the data into train test and validation
3: **for** $i = 1$ to 6 **do**
  Train the model M_i on the training data;
  Evaluate the performance of model M_i on the validation set and test set;
4: **end for**
5: **Sort** the models M_1 to M_6 based on their evaluation scores S_i in descending order, such that:
  $\forall 1 \leq k \leq 6 \ |\{i \in \{1, 2, 3, 4, 5, 6\} \mid S_i = S_k\}|$
6: **Select** the two best-performing models:
  $BM\_1 = \max\{M_i \mid M_i \in \{M_1, M_2, M_3, M_4, M_5, M_6\}\}$
  $BM\_2 = \max\{M_i \mid M_i \in \{M_1, M_2, M_3, M_4, M_5, M_6\}$ and $M_i \neq BM\_1\}$
7: **Load** two optimal models: BM_1 and BM_2 from the sorted list;
8: **Assign** custom weights for models:
  $custom_{weight} = [x, y]$ & $(x + y) = 1$;
9: **if** BM_1accuracy $>$ BM_2accuracy **then**
10: $x > y$;
11: **end if**
12: **Create** model input:
  $Input$ = Input(shape=(Height, Width, 3));
  $Pred_{BM1} = BM_1(Input)$;
  $Pred_{BM2} = BM_2(Input)$;
13: **Compute ensemble model prediction using custom weights:**
  $E\_Pred = \sum_{i=1}^{2}(Pred_{BMi} \times custom_{weight}[i])$;
14: **return** E_Pred;

In the weighted ensemble process, custom weights, x and y were assigned to each model, giving more weight to the more accurate model. Subsequently, the input was passed through the model both BM_1 and BM_2, by generating individual model predictions as $Pred_{BM1}$ and $Pred_{BM2}$. These predictions are then combined using the assigned weights, resulting in the final ensemble prediction, generating the final prediction, denoted as E_{pred}. This weighted average effectively captured the strengths of both models while emphasizing each model's contribution. This process is demonstrated in lines 12 and 13 of Algorithm 1 and Fig. 5.

B. OPTIMIZATION STRATEGIES

In our study, the Adam optimizer was used as the optimization technique. The Adam optimizer is a first-order gradient-based

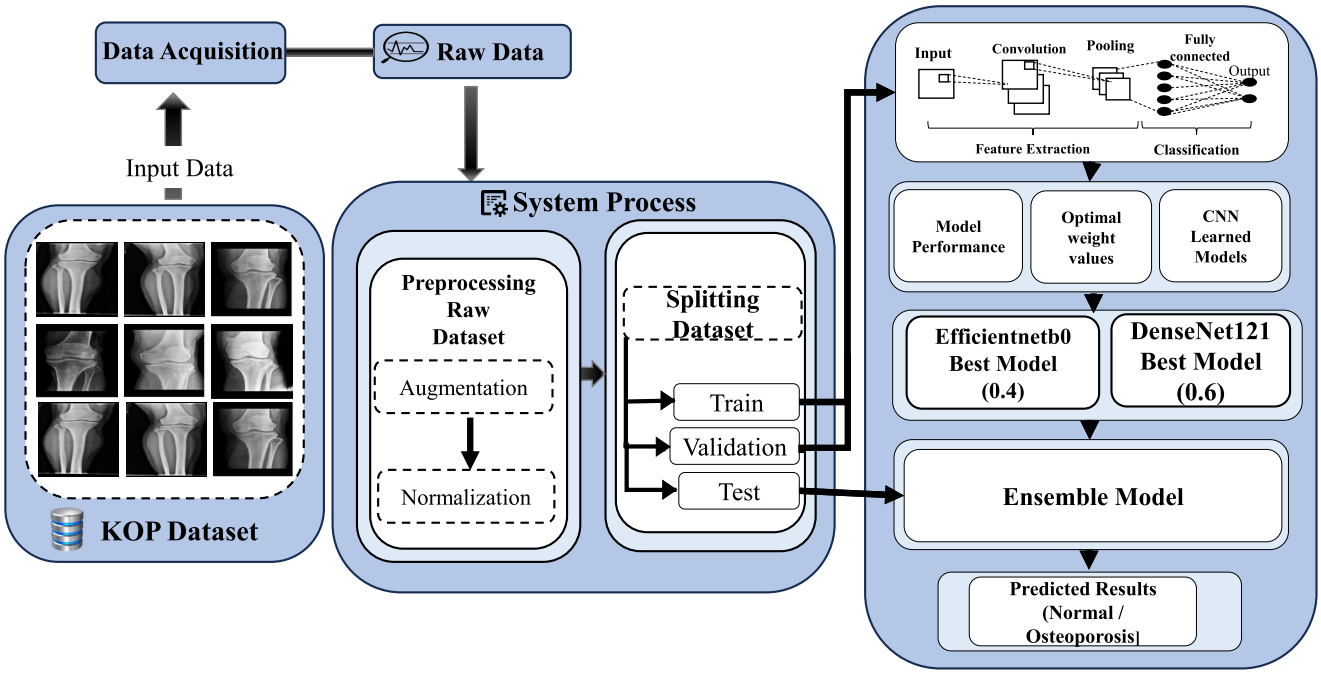

FIGURE 5. Illustration of our proposed approach for KOP classification. The diagram depicts the key components and workflow of our KONet model.

optimization algorithm that utilizes a stochastic objective function based on the adaptive estimation of low-order moments. The Adam optimizer was used owing to its fast convergence in classification tasks compared to other optimization techniques [46], which is achieved by maintaining separate learning rates for each weight in the network and adapting these learning rates to past gradients. This process results in rapid convergence to optimal weights. The Adam optimizer compares favorably with other optimization methods, tools, and random devices [47]. This algorithm is used to accelerate the gradient reduction algorithm through an exponentially weighted average of the gradients, whereby the algorithm reaches the minimum faster.

V. MATERIALS AND EXPERIMENTAL SETUP

This section provides a comprehensive description of the data preprocessing methods and experimental setup.

A. DATASET

In this study, we utilized the publicly available osteoporosis knee X-ray dataset from Kaggle [31]. This dataset, which contains normal and osteoporotic classes, consists of 372 images. Some examples are shown in Figure 1. Compared to other medical image datasets, the KOP image datasets are not widely and publicly available, with the dataset mentioned in [31] being the sole exception. Considering this obstacle, we conducted our study using the dataset mentioned in [31].

1) DATA PREPROCESSING

Initially, data preprocessing was performed in three steps: resizing, augmentation, and data splitting. The dataset contained images of different sizes. As an initial step, we resized the image to $Image^{Height \times Width \times 3}$ according to the input size. Next, data augmentation was conducted to increase the size of the dataset, using the Augmentor library. Data augmentation not only helps prevent overfitting but also improves generalization and reduces bias, thereby improving model performance on unseen data. The dataset size was increased to 4000 images. Rotation, shear, and zooming methods were used to augment the images. Examples of the augmented data are shown in Figure 6.

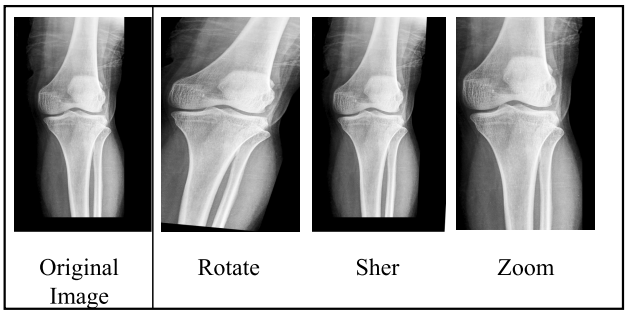

FIGURE 6. Comparative analysis between the original image and augmented samples from the KOP dataset.

Subsequent to data augmentation, normalization was applied, mostly to minimize the influence of lighting condition variations on the images. This method can enhance the adaptability of the model. The data were then divided into three parts: training, validation, and testing in the ratio of 0.8, 0.1, and 0.1, respectively. The Python library "split-folder" was used to perform the data-splitting.

B. EXPERIMENTAL SETUP

The study was carried out in the Keras framework using the features provided in the Colab Pro environment. The experimental method involved numerous steps, including training, validation, and testing, all performed on a Tesla T4 GPU processing unit. The Keras framework was chosen because of the wide support it offers for deep learning tasks and its user-friendly interface, enabling rapid and successful model creation. This decision provided access to an extensive library of pre-implemented neural network topologies, optimization methods, and assessment measures. All of our constructed networks were trained with a batch size of 32, and the number of training epochs was set to 40.

VI. DISCUSSION

A. PERFORMANCE METRICS ANALYSIS

This section provides the performance indicators utilized for evaluating the qualitative and quantitative effectiveness of our approach.

1) CONFUSION MATRIX ANALYSIS

In statistics, true positive T_P (refers to the model predicting a positive result, when the actual result is also positive. True negative T_N refers to the model predicting a negative result when the actual result is also negative. False negative F_N refers to the model predicting a negative result when the actual result is positive. Finally, false positive $F_P$refers to the model predicting a positive result when the actual result is negative [47], [48].

According to the findings presented in Figure 7, the confusion matrix for the proposed model displays the relationship between the actual and predicted values for the classification classes. The plot on the right shows that T_p is 205; $Fp$is 10; $F_n$is 1; and $T_n$is 183. The plots on the left show these values as percentages, corresponding to a T_p of 51.38%, F_p of 2.51%, F_n of 0.25%, and T_n of 45.85%.

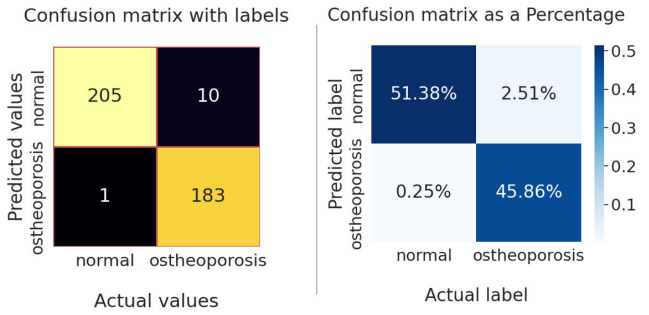

FIGURE 7. Confusion matrix comparison of the KONet.

2) ACCURACY

Accuracy is a measure of how often a classification model correctly predicts items, as shown in Eq. 3 to evaluate the effectiveness of the proposed approach.

$$Accuracy = \frac{T_p + T_n}{T_p + T_n + F_p + F_n} \tag{3}$$

Figure 8 illustrates the accuracy of each model during the training (blue line) and validation (orange line) phases. The performance of DenseNet121 is presented in Figure 8(a) During the training phase, initially an upward trend is observed; however, after the 5th epoch, a constant level is maintained as a straight line. The validation line remains consistently above the training line and is slightly noisier. In Figure 8(b), the training and validation accuracy values of EfficientNetB0, start at higher values than those of

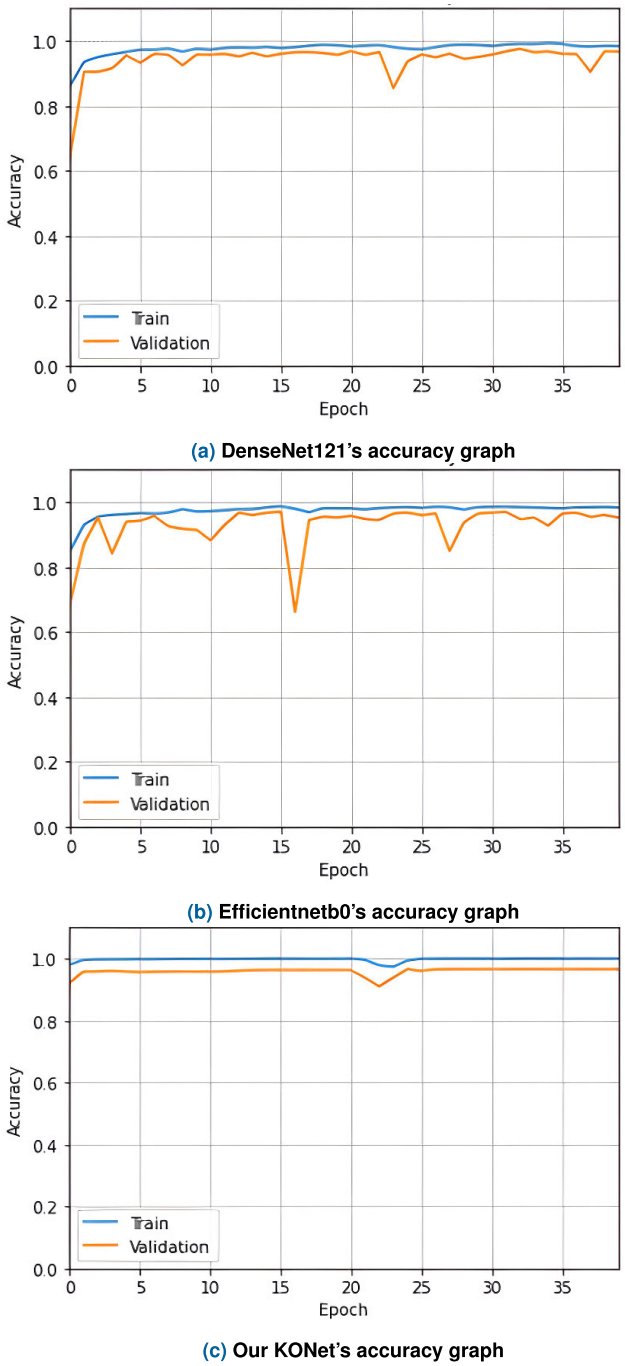

FIGURE 8. Comparison of KONet and other well performing models on training and validation accuracy.

DenseNet121 and exhibit an upward trend. The gap between training and validation accuracy is comparatively higher than that in DenseNet121. In Figure 8(c), the graph depicts the accuracy of KONet, starting with good training and validation values. The lines for KONet display a smooth approach to all the training and validation phases. In the 21st epoch, the best validation value for all three methods is attained.

3) PRECISION, RECALL, AND F1-SCORE

Precision and Recall are useful measures of success prediction when the classes are highly imbalanced [47]. Precision is the ratio of what a model classifies as true to what is actually true, as expressed in Eq. (4):

$$Precision = \frac{T_p}{T_p + F_p} \tag{4}$$

In addition to precision, recall is also used to indicate success or hit rate. Recall is the ratio of what the model predicts versus reality, and is expressed as in Eq.(5):

$$Recall = \frac{T_p}{T_p + F_n} \tag{5}$$

The F1 score is a good performance metric for binary classification tasks. In the case of two classes such as positive and negative, F1 is the harmonic mean of precision and recall. The F1 score is expressed in Eq. (6):

$$F1score = 2 \times \frac{Precision \times Recall}{Precision + Recall} \tag{6}$$

In Table 2, precision, recall, and F1-score are displayed. Among these, the proposed ensemble model, KONet, performs better than the other models. Here, the values were calculated using the Marco average to average multiclass values. These values are calculated with the support of 399 images.

TABLE 2. Review of the performance of various models on the KOP dataset. The metrics evaluated include precision, recall, and F1-score for each model.

MODEL	PRECISION	RECALL	F1-SCORE
Densenet-121	0.96	0.96	0.96
EfficientNetb0	0.95	0.95	0.95
Resnet50	0.87	0.87	0.87
Vgg-19	0.88	0.88	0.88
MobileNet	0.95	0.95	0.95
Our KONet	**0.97**	**0.97**	**0.97**
Inception V3	0.94	0.94	0.94

Table 3 displays the class-wise performances of the proposed model. According to this table, the normal class has the highest precision of 1.00, whereas the osteoporotic class has the highest recall value.

In this study, we evaluated the performance of the proposed ensemble model and other well-known models, such as Resnet50, VGG-19, DenseNet121, MobileNet, EfficientNetB0, and InceptionV3, that achieved better performance on the ImageNet dataset.

TABLE 3. Class-wise performance evaluation review of the KOP dataset. The metrics include precision, recall, and F1-score for each class (normal and osteoporosis).

CLASSES	PRECISION	RECALL	F1-SCORE
Normal	**1.00**	0.95	**0.97**
Osteoporosis	0.95	**0.99**	**0.97**

According to Table 4, in terms of training accuracy, the performance of InceptionV3 is impressive. However, the validation and testing accuracy is significantly lower than that of the proposed KONet, and the validation and testing loss is relatively high. This is because InceptionV3 uses a combination of convolutional layers with modules, whereas EfficientNet and DenseNet use skip connections allowing the reuse of features, which leads to better performance, alongside the proposed model in terms of validation and testing accuracy with respect to InceptionV3. In addition, InceptionV3 required more computation time than the other networks during the training phase. Resnet50 and Vgg-19 performed worse than the other networks because these networks are simpler than the others. ResNet-50 (50 layers) and VGG-19 (19 layers) have fewer layers than the other networks, which is another reason for the reduced training time consumed per epoch by these networks. Table 4 clearly shows that our proposed KONet outperforms the other models in the testing and validation phases with a significant margin of 1%, while having the second-highest number of parameters.

The visual representation in figure 9 depicts a bubble chart of the model performances, along with time consumption per epoch. It's evident that Inceptionv3 exhibits a significantly

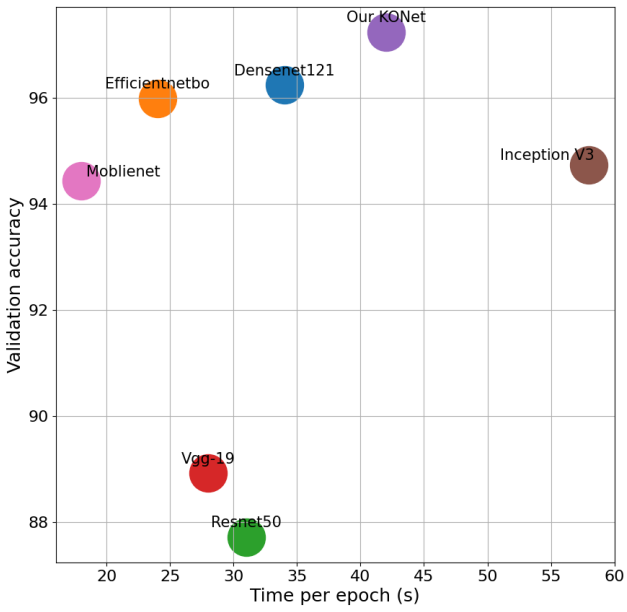

FIGURE 9. Comparison of model performance and time per epoch (in seconds).

TABLE 4. In-depth analysis of model accuracy on the KOP dataset.

MODELS	TRAIN ACCURACY	VALIDATION ACCURACY	TRAIN LOSS	VALIDATION LOSS	TEST ACCURACY	EPOCHS	TIME PER EPOCH	PARAMETERS
Densenet121	0.9703	0.9624	0.0751	0.1175	0.9562	40	34(s)	7563330
Mobilenet	0.9787	0.9474	0.0532	0.1687	0.9434	40	18(s)	3754690
EfficientNetb0	0.9734	0.9599	**0.0248**	0.2010	0.9576	40	24(s)	22852898
Resnet50	0.9041	0.8772	0.2232	0.4487	0.8881	40	31(s)	24637826
Vgg19	0.9296	0.8897	0.2109	0.3322	0.9104	40	28(s)	20288066
Our KONet	0.9794	**0.9724**	0.0458	**0.0897**	**0.9652**	40	42(s)	30251652
InceptionV3	**0.9806**	0.9474	0.0455	0.1776	0.9378	40	58(s)	52852898

TABLE 5. Performance accuracy of different DenseNet121 and EfficientNetB0 ratios on the KOP dataset. The ratios indicate the relative contributions of the two models in a weighted ensemble.

DenseNet121 ratio	EfficientNetB0 ratio	Train accuracy	Validation accuracy	Train loss	Validation loss	Test accuracy
0.9	0.1	0.9878	0.9584	0.1229	0.4520	0.9504
0.8	0.2	**0.9894**	0.9599	**0.0126**	0.4159	0.9514
0.7	0.3	0.9878	0.9524	0.0229	0.4720	0.9540
0.6	0.4	0.9794	**0.9724**	0.0458	**0.0897**	**0.9652**
0.5	0.5	0.9787	0.9574	0.0502	0.2284	0.9610
0.4	0.6	0.9747	0.9449	0.0531	0.3002	0.9510
0.3	0.7	0.9759	0.9440	0.0526	0.3032	0.9502
0.2	0.8	0.9703	0.9474	0.0631	0.3879	0.9492
0.1	0.9	0.9683	0.9450	0.0729	0.3974	0.9486

higher computation time than its peers and has a comparatively inferior validation accuracy. Despite having the second-highest training time per epoch, our proposed KONet outperforms other models in terms of validation accuracy by a considerable margin. This is because the weights assigned to Densenet121 and EfficientNetB0 (0.6 and 0.4, respectively) constrain their contributions to the ensemble prediction.

To select the suitable weight ratios, we conducted experiments using various ratios of Densenet121 and EfficientNetB0. The corresponding results are presented in Table 5. Densenet121 (0.6) and EfficientNetB0 (0.4) provided better results compared to the other weight ratios during validation and testing.

In addition, several images were tested using the proposed model. Four test results from the test data are displayed. Two images from each designated class and the proposed model successfully distinguish the images with respect to the ground truth. Figure 10 shows the predicted outputs categorized according to ground truth.

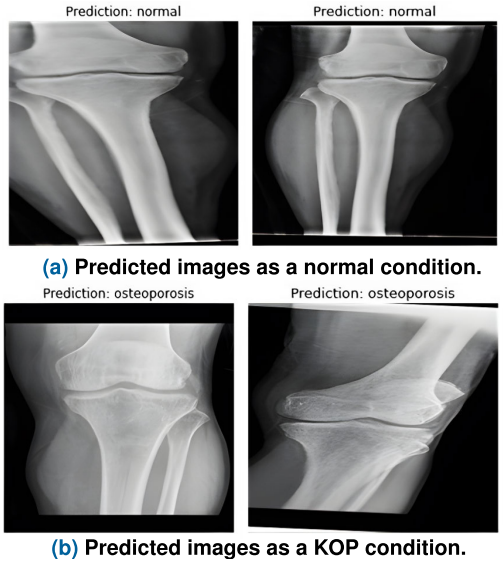

FIGURE 10. Visual analysis of test results: comparison of four test images using the proposed KONet.

B. COMPREHENSIVE DISCUSSION OF THE ADVANTAGES AND LIMITATIONS OF THE KONet MODEL

Our proposed KONet model has demonstrated superior performance in the KOP classification task. This is achieved by combining the EfficientNetB0 and DenseNet121 models, weighted according to their individual performance. This approach allows KONet to effectively leverage the strengths of these individual models while mitigating their limitations. Even minor improvements in accuracy have significant implications for contemporary disease detection and the diagnosis of patients, highlighting the significance of our findings.

The primary limitation of our study is that the KONet model utilizes more parameters compared to the DenseNet121 and EfficientNetB0 models. Nonetheless, our research offers valuable insights into the potential advantages of using a weighted ensemble approach to enhance the accuracy of KOP classification. We recommend that future studies explore alternative methods to reduce the number of parameters without compromising performance. Nevertheless, our findings underscore the importance of employing a weighted ensemble approach to achieve high accuracy in KOP classification tasks.

VII. CONCLUSION

The severity of KOP warrants timely diagnosis and assessment; however, relying on human experts can be time-consuming and costly. The aid offered by visual AI plays a pivotal role in making informed decisions regarding images acquired from various patients. This study employed an ensemble model that uses the concatenation of two transfer-learning models to classify KOP. The proposed method achieved promising results compared with other state-of-the-art models. Consequently, this model can help clinicians diagnose KOP at a low cost. A limitation of this study is that the performance of the ensemble model is significantly affected by the choice of the base classifier. The accuracy of the model can be further improved by introducing an attention mechanism focused on the channel-wise importance of deep features of KOP images, which will be explored in future research.

DECLARATIONS AND STATEMENTS

DATA AVAILABILITY STATEMENT

The datasets used and/or analyzed during the current study are available from the corresponding author upon reasonable request.

REFERENCES

[1] T. S. Yang, "Recognition and classification of knee osteoporosis and osteoarthritis severity using deep learning techniques," Ph.D. dissertation, Nat. College Ireland, Dublin, Ireland, 2022.

[2] O. Johnell and J. A. Kanis, "An estimate of the worldwide prevalence and disability associated with osteoporotic fractures," *Osteoporosis Int.*, vol. 17, no. 12, pp. 1726–1733, Oct. 2006.

[3] H. Kato, A. J. Ansh, E. R. Lester, Y. Kinoshita, N. Hidaka, Y. Hoshino, M. Koga, Y. Taniguchi, T. Uchida, and H. Yamaguchi, "Identification of enpp1 haploinsufficiency in patients with diffuse idiopathic skeletal hyperostosis and early-onset osteoporosis," *J. Bone Mineral Res.*, vol. 37, no. 6, pp. 1125–1135, 2022.

[4] I. M. Wani and S. Arora, "Computer-aided diagnosis systems for osteoporosis detection: A comprehensive survey," *Med. Biol. Eng. Comput.*, vol. 58, no. 9, pp. 1873–1917, Sep. 2020.

[5] H.-W. Chang, Y.-H. Chiu, H.-Y. Kao, C.-H. Yang, and W.-H. Ho, "Comparison of classification algorithms with wrapper-based feature selection for predicting osteoporosis outcome based on genetic factors in a Taiwanese women population," *Int. J. Endocrinol.*, vol. 2013, pp. 1–8, Jan. 2013.

[6] S. Gnudi, E. Sitta, and L. Lisi, "Relationship of body mass index with main limb fragility fractures in postmenopausal women," *J. Bone Mineral Metabolism*, vol. 27, no. 4, pp. 479–484, Jul. 2009.

[7] J. Kanis, P. Delmas, J. Reeve, P. Garnero, A. Tenenhouse, J. Melton, A. Oden, E. McCloskey, H. Pols, and C. De Laet, "A meta-analysis of previous fracture and fracture risk," *Bone*, vol. 32, no. 5, p. S84, 2003.

[8] N. T. Chung, P. H. Van, N. M. Tri, L. T. Tuyet, N. D. Thuan, and T. V. Binh, "Pain relief effect of TT knee remedy on knee osteoporosis," *Med. Sci.*, vol. 24, no. 104, pp. 2531–2536, 2020.

[9] S. R. Cummings and L. J. Melton, "Epidemiology and outcomes of osteoporotic fractures," *Lancet*, vol. 359, no. 9319, pp. 1761–1767, May 2002.

[10] Y. Oishi, Y. Hirano, Y. Hasegawa, K. Yamauchi, Y. Kanayama, and S. Ota, "Prior knee osteoporosis associating the 10-year clinical outcome of total knee arthroplasty for rheumatoid arthritis: A retrospective study," *J. Musculoskeletal Res.*, vol. 20, no. 2, Jun. 2017, Art. no. 1750007.

[11] W. Gouda, M. Almurafeh, M. Humayun, and N. Z. Jhanjhi, "Detection of COVID-19 based on chest X-rays using deep learning," *Healthcare*, vol. 10, no. 2, p. 343, Feb. 2022.

[12] A. D. Brett and J. K. Brown, "Quantitative computed tomography and opportunistic bone density screening by dual use of computed tomography scans," *J. Orthopaedic Transl.*, vol. 3, no. 4, pp. 178–184, Oct. 2015.

[13] Y. Chen, C.-B. Schönlieb, P. Lió, T. Leiner, P. L. Dragotti, G. Wang, D. Rueckert, D. Firmin, and G. Yang, "AI-based reconstruction for fast MRI—A systematic review and meta-analysis," *Proc. IEEE*, vol. 110, no. 2, pp. 224–245, Feb. 2022.

[14] Y. Chen, Y. Guo, X. Zhang, Y. Mei, Y. Feng, and X. Zhang, "Bone susceptibility mapping with MRI is an alternative and reliable biomarker of osteoporosis in postmenopausal women," *Eur. Radiol.*, vol. 28, no. 12, pp. 5027–5034, Dec. 2018.

[15] I. M. Wani and S. Arora, "Osteoporosis diagnosis in knee X-rays by transfer learning based on convolution neural network," *Multimedia Tools Appl.*, vol. 82, no. 9, pp. 14193–14217, Apr. 2023.

[16] U. B. Abubakar, M. M. Boukar, and S. Adeshina, "Comparison of transfer learning model accuracy for osteoporosis classification on knee radiograph," in *Proc. 2nd Int. Conf. Comput. Mach. Intell. (ICMI)*, Jul. 2022, pp. 1–5.

[17] U. B. Abubakar, M. M. Boukar, and S. Adeshina, "Evaluation of parameter fine-tuning with transfer learning for osteoporosis classification in knee radiograph," *Int. J. Adv. Comput. Sci. Appl.*, vol. 13, no. 8, 2022.

[18] T. Rahman, M. E. H. Chowdhury, A. Khandakar, K. R. Islam, K. F. Islam, Z. B. Mahbub, M. A. Kadir, and S. Kashem, "Transfer learning with deep convolutional neural network (CNN) for pneumonia detection using chest X-ray," *Appl. Sci.*, vol. 10, no. 9, p. 3233, May 2020.

[19] Y. Chen, Q. Zhang, Y. Wu, B. Liu, M. Wang, and Y. Lin, "Fine-tuning resnet for breast cancer classification from mammography," in *Proc. 2nd Int. Conf. Healthcare Sci. Eng.* Cham, Switzerland: Springer, 2019, pp. 83–96.

[20] A. Chattopadhyay and M. Maitra, "MRI-based brain tumour image detection using CNN based deep learning method," *Neurosci. Informat.*, vol. 2, no. 4, Dec. 2022, Art. no. 100060.

[21] E. S. Olivas, J. D. M. Guerrero, M. Martinez-Sober, J. R. Magdalena-Benedito, and L. Serrano, *Handbook of Research on Machine Learning Applications and Trends: Algorithms, Methods, and Techniques: Algorithms, Methods, and Techniques*. Hershey, PA, USA: IGI Global, 2009.

[22] X. Yu, J. Wang, Q.-Q. Hong, R. Teku, S.-H. Wang, and Y.-D. Zhang, "Transfer learning for medical images analyses: A survey," *Neurocomputing*, vol. 489, pp. 230–254, Jun. 2022.

[23] A. Farooq, S. Anwar, M. Awais, and S. Rehman, "A deep CNN based multi-class classification of Alzheimer's disease using MRI," in *Proc. IEEE Int. Conf. Imag. Syst. Techn. (IST)*, Oct. 2017, pp. 1–6.

[24] P. Rajpurkar, J. Irvin, K. Zhu, B. Yang, H. Mehta, T. Duan, D. Ding, A. Bagul, C. Langlotz, and K. Shpanskaya, "CheXNet: Radiologist-level pneumonia detection on chest X-rays with deep learning," 2017, *arXiv:1711.05225*.

[25] S. Pereira, A. Pinto, V. Alves, and C. A. Silva, "Brain tumor segmentation using convolutional neural networks in MRI images," *IEEE Trans. Med. Imag.*, vol. 35, no. 5, pp. 1240–1251, May 2016.

[26] X. Zhang and S.-G. Zhao, "Fluorescence microscopy image classification of 2D HeLa cells based on the CapsNet neural network," *Med. Biol. Eng. Comput.*, vol. 57, no. 6, pp. 1187–1198, Jun. 2019.

[27] S. Sukegawa, A. Fujimura, A. Taguchi, N. Yamamoto, A. Kitamura, R. Goto, K. Nakano, K. Takabatake, H. Kawai, H. Nagatsuka, and Y. Furuki, "Identification of osteoporosis using ensemble deep learning model with panoramic radiographs and clinical covariates," *Sci. Rep.*, vol. 12, no. 1, p. 6088, Apr. 2022.

[28] S. Ahmad, J.-S. Kim, D. K. Park, and T. Whangbo, "Automated detection of gastric lesions in endoscopic images by leveraging attention-based YOLOv7," *IEEE Access*, vol. 11, pp. 87166–87177, 2023.

[29] A. Konwer, X. Xu, J. Bae, C. Chen, and P. Prasanna, "Temporal context matters: Enhancing single image prediction with disease progression representations," in *Proc. IEEE/CVF Conf. Comput. Vis. Pattern Recognit. (CVPR)*, Jun. 2022, pp. 18802–18813.

[30] (Mar. 27, 2023). *(Year of Publication or Data Release) Knee X-ray Osteoporosis Database*. [Online]. Available: https://data.mendeley.com/datasets/fxjm8fb6mw/2

[31] StevePython. (2021). *Osteoporosis Knee Xray Dataset*. Accessed: Feb. 10, 2023. [Online]. Available: https://www.kaggle.com/datasets/stevepython/osteoporosis-knee-xray-dataset

[32] K. Hatano, S. Murakami, H. Lu, J. K. Tan, H. Kim, and T. Aoki, "Classification of osteoporosis from phalanges CR images based on DCNN," in *Proc. 17th Int. Conf. Control, Autom. Syst. (ICCAS)*, Oct. 2017, pp. 1593–1596.
[33] K. Weiss, T. Khoshgoftaar, and D. Wang, "A survey of transfer learning," *J. Big Data*, vol. 3, pp. 1–40, May 2016.
[34] H. E. Kim, A. Cosa-Linan, N. Santhanam, M. Jannesari, M. E. Maros, and T. Ganslandt, "Transfer learning for medical image classification: A literature review," *BMC Med. Imag.*, vol. 22, no. 1, p. 69, Dec. 2022.
[35] Y. Hao, "Convolutional neural networks for image classification," in *Proc. 2nd Int. Conf. Artif. Intell. Comput. Eng. (ICAICE)*, Nov. 2021, pp. 342–345.
[36] F.-F. Li, J. Johnson, and S. Yeung. (2017). *CS231N: Convolutional Neural Networks for Visual Recognition*. Accessed: Sep. 2022. [Online]. Available: http://cs231n.stanford.edu/2017/
[37] D. Ezzat and H. A. Ella, "GSA-DenseNet121-COVID-19: A hybrid deep learning architecture for the diagnosis of COVID-19 disease based on gravitational search optimization algorithm," 2020, *arXiv:2004.05084*.
[38] OpenGenus IQ. (2019). *Architecture of DenseNet121*. Accessed: Feb. 2023. [Online]. Available: https://iq.opengenus.org/architecture-of-densenet121/
[39] S. Nandhini and K. Ashokkumar, "An automatic plant leaf disease identification using DenseNet-121 architecture with a mutation-based Henry gas solubility optimization algorithm," *Neural Comput. Appl.*, vol. 34, no. 7, pp. 5513–5534, Apr. 2022.
[40] B. Koonce and B. Koonce, "EfficientNet," in *Convolutional Neural Networks With Swift for Tensorflow: Image Recognition and Dataset Categorization*, 2021, pp. 109–123.
[41] A. S. Ebenezer, S. D. Kanmani, M. Sivakumar, and S. J. Priya, "Effect of image transformation on EfficientNet model for COVID-19 CT image classification," *Mater. Today, Proc.*, vol. 51, pp. 2512–2519, 2022.
[42] D. Xue, X. Zhou, C. Li, Y. Yao, M. M. Rahaman, J. Zhang, H. Chen, J. Zhang, S. Qi, and H. Sun, "An application of transfer learning and ensemble learning techniques for cervical histopathology image classification," *IEEE Access*, vol. 8, pp. 104603–104618, 2020.
[43] D. A. P. Hooftman, J. M. Bullock, L. Jones, F. Eigenbrod, J. I. Barredo, M. Forrest, G. Kindermann, A. Thomas, and S. Willcock, "Reducing uncertainty in ecosystem service modelling through weighted ensembles," *Ecosystem Services*, vol. 53, Feb. 2022, Art. no. 101398.
[44] F. Zhao, G.-Q. Zeng, and K.-D. Lu, "EnLSTM-WPEO: Short-term traffic flow prediction by ensemble LSTM, NNCT weight integration, and population extremal optimization," *IEEE Trans. Veh. Technol.*, vol. 69, no. 1, pp. 101–113, Jan. 2020.
[45] K.-D. Lu, Z.-G. Wu, and T. Huang, "Differential evolution-based three stage dynamic cyber-attack of cyber-physical power systems," *IEEE/ASME Trans. Mechatronics*, vol. 28, no. 2, pp. 1137–1148, Apr. 2023.
[46] S. Mehta, C. Paunwala, and B. Vaidya, "CNN based traffic sign classification using Adam optimizer," in *Proc. Int. Conf. Intell. Comput. Control Syst. (ICCS)*, May 2019, pp. 1293–1298.
[47] J.-A. Ting, S. Vijayakumar, and S. Schaal, *Encyclopedia of Machine Learning*. Cham, Switzerland: Springer, 2010, pp. 613–624.
[48] Kharshit. (Dec. 2018). *Loss vs Accuracy*. Accessed: Feb. 2023. [Online]. Available: https://kharshit.github.io/blog/2018/12/07/loss-vs-accuracy

M. J. AASHIK RASOOL (Member, IEEE) received the B.Sc. degree in computer engineering from Gachon University, South Korea, in 2022, where he is currently pursuing the master's degree in computer engineering. His research interests include artificial intelligence, deep reinforcement learning, super-resolution, computer vision, AI in healthcare, natural language processing, and large language models.

SHABIR AHMAD (Senior Member, IEEE) received the B.S. degree in computer system engineering from the University of Engineering and Technology, Peshawar, Pakistan, the M.S. degree in computer software engineering from the National University of Sciences and Technology, Islamabad, Pakistan, in 2013, and the Ph.D. degree from the Department of Computer Engineering, Jeju National University, Republic of Korea. He was a Faculty Member with the Software Engineering Department, University of Engineering and Technology, from 2016 to 2022. He is currently a Research Professor with the Department of Content Technology Development and Game Engineering, Gachon University. His research work mainly focused on the Internet of Things applications, cyber-physical systems, intelligent systems, deep learning, and reinforcement learning.

UMIRZAKOVA SABINA received the bachelor's degree from the Tashkent University of Information Technology, Uzbekistan, in 2015, and the master's and Ph.D. degrees from the Department of IT Convergence Engineering, Gachon University, Republic of Korea, in 2019 and 2021, respectively. She is currently an Assistant Professor with the Department of IT Convergence Engineering, Gachon University. Her research interests include but not limited to medical imaging, smart healthcare, and image and face segmentation using state-of-the-art deep learning solutions.

TAEG KEUN WHANGBO (Member, IEEE) received the M.S. degree in computer sciences from The City University of New York, in 1988, and the Ph.D. degree in computer sciences from the Stevens Institute of Technology, in 1995. Currently, he is a Professor with the Department of Computer Science, Gachon University, South Korea. Before he joined Gachon University, he was a Software Developer with Q-Systems, Englewood Cliffs, NJ, USA, from 1988 to 1993. He was a Researcher with Samsung Electronics, from 2005 to 2007. His research interests include computer graphics, HCI, and VR/AR. From 2006 to 2008, he was the President of the Association of Korean Cultural Technology.